Chapter

Two-Dimensional MXene Based Materials for Micro-Supercapacitors

Aditya Sharma and Chandra Sekhar Rout

Abstract

With the boom in the development of micro-electronics for wearable and flexible electronics, there is a growing demand for micro-batteries and micro-supercapacitors (MSCs). Micro-supercapacitors have garnered a considerable attention for the evolution of these energy storage micro-systems. The choice of electrode material plays a pivotal role in the fabrication and development of MSCs. Recently, a new emerging family of two-dimensional transition metal (M) carbides or nitrides (X) cited as 2D MXene has emerged as a novel material. Due to its exceptionally high electronic conductivity ~10,000 S cm^{-1}, high charge storage capacity and easy processing capability helps to use MXene as the promising candidate for micro-supercapacitors electrodes. Taking the advantage of such exceptional properties. MXenes have been explored enormously in stacked as well as in interdigital architecture for on-chip micro-supercapacitors (MSCs). This book chapter includes a recent advancement of MXene based MSCs, with a brief overview of synthesis and fabrication techniques.

Keywords: 2D MXene, Micro-supercapacitor, Wearable and flexible electronics, Energy storage, Micropattern

1. Introduction

There is an increase in demand for flexible and solid-state on chip micro-electronics for smart wearable micro-devices for energy, environmental, biological, medical and various other applications which can be either wireless or integrated with solar or piezoelectric energy harvesters. Great efforts have been made by the scientists to design and develop smart as well as portable microsystems, primarily for self-powered and on-chip integrated power systems. To cope with the increasing demand of micro-electronics, there is an abrupt rise in the demand of micro-energy storage devices. However, micro-batteries are restricted due to their limited life and power density. Micro-supercapacitors (MSCs) hold the best alternate to the micro-batteries, despite the lower energy density. In contrast, MSCs can demonstrate superior cycle life, faster charge/discharge rates, high power density as well as overall stable performance which is promising [1]. Presently, MSCs have two types of architecture, one with the conventional sandwich type and others are in-plane interdigital pattern type as shown in **Figure 1(a, b)**, [2]. Generally, the interdigitated coplanar design offers better performance due to the short ion diffusion distance which gives the enormous surface area. Thus, exhibiting an excellent rate capability, high-power density and ease of integration with micro-devices [1, 4, 5].

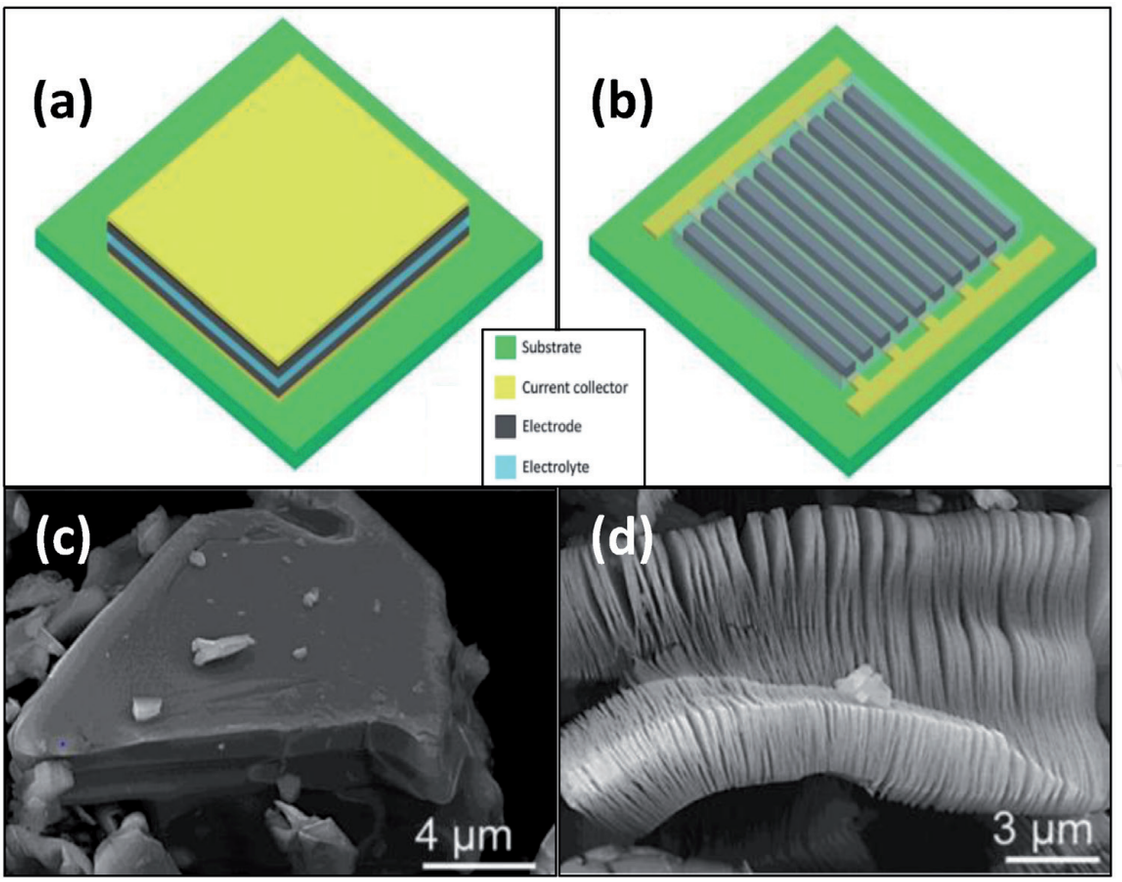

Figure 1.
Architecture of micro-supercapacitors: (a) sandwich type micro-supercapacitor, (b) interdigital patterned micro-supercapacitor. [2] (c) SEM image of Ti_3AlC_2 (MAX) phase, (d) SEM image of etched $Ti_3C_2T_x$ (MXene) phase [3].

Two-dimensional (2D) materials like graphene, h-BN, Transition metal dichalcogenides (TMDCs), black phosphorus (BP), MXenes and 2D metal oxides and hydroxides etc. are most widely used in energy storage applications due to their outstanding electronic, mechanical, optical and physio-chemical properties [6]. Carbon based materials including Carbon [7], carbide derived carbon [8], onion-like carbon [9], graphene [10], Carbon nano tubes (CNT) [11], laser scribed graphene [12] displays high electronic conductivity and relatively large surface area but due to electric double layer formation, they lack high energy density. Similarly, pseudocapacitive materials such as transition metal oxides like MnO_2 [13], MoO_3 [14], conductive polymers [15] as well as TMDs [16] which suffer from low electronic conductivity with reasonable power and cycling performance has been already explored in Micro-supercapacitor devices applications. But, MXenes have garnered great attention from the scientific community all over the world since their discovery in 2011, by Naguib and group [17]. A large family of two-dimensional early carbides, nitrides and carbon nitrides produced by selective etching of A layer (typically Al and Ga) from the precursor layered ternary carbides/nitrides (MAX phases). Their general formula is $M_{n+1}X_nT_X$ (n = 1, 2, 3), where M represents a Transition metal, X is carbon and/or nitrogen, T stands for surface termination groups (-F, -OH, -O etc.) [18]. In particular, the dual nature of MXenes that is superior ion transport due to inner transition metal carbide layer as well as property to exhibit fast redox reaction because of large active sites [18, 19]. MXenes combine high electronic conductivity of MAX phases as well as hydrophilic nature due to the surface terminations such properties make them a considerable candidate for a host of applications. $Ti_3C_2T_X$ is one of the most studied member of

MXene family, exhibiting a high electronic conductivity up to~2.4 × 10^4 S/cm and volumetric capacitance 1500 F/cm^3 with good rate capability of 10 V/s in acidic electrolyte [5]. Hence there is plenty of room to design and develop MXene based Micro-supercapacitor devices [20]. The 2D nature, excellent mechanical stability and exceptionally tunable physio-chemical properties makes MXenes, the best candidate for MSC device. This book chapter includes various direct–indirect techniques to fabricate MXene based MSC device.

2. MXenes: brief review

2.1 Synthesis

There are generally two methods to synthesize MXene i.e., (1) top-down approach which includes selective etching or exfoliation of metal layer and (2) bottom-up approach including chemical vapor deposition (CVD), template assisted growth method. Wet chemical etching i.e., fluoride based acids are most commonly reported methods to etch "A" element, generally group IIIA and IVA group (Al or Si) elements from MAX phases (one or several atomic layers) which are replaced by functional groups, where M is termed as early transition metals, from group IIIB to IVB, and X is carbide/nitride by using different wt % of fluoride containing acid such as HF or mixture of LiF-HCl acid [17, 20, 21]. The first ever report to synthesis MXene by eliminating the aluminium layer from Ti_3AlC_2 (MAX) by using hydrogen fluoride (HF) in the range of 10 to 50 % concentration of etchant [17]. The exfoliated 2D $Ti_3C_2T_x$ possess excellent 2D sheets like morphology almost similar to graphene sheets as shown in **Figure 1(c,d)** [3]. To avoid highly acidic HF acid, various other methods have been developed to produce in-situ HF salts comparatively less hazardous than HF. Recently, a new approach to etch with molten salts allows to dissolve A-element at high temperature [21]. This method demonstrated the complete removal of Fluorine ions and found to be much purer MXene than one etched with only HF. The presence of surface functional groups like -OH, -F and -O etc. improves the hydrophilic character of MXenes which further enhances the stability. The reaction mechanism of firstly synthesized $Ti_3C_2T_X$ (MXene) by etching Al layers from Ti_3AlC_2 (MAX phase) with HF is given in **Figure 2(a)** [22].

$$Ti_3AlC_2 + 3\mathrm{HF} = AlF_3 + 3/2\,\mathrm{H}_2 + Ti_3\mathrm{C}_2 \quad (1)$$

$$Ti_3\mathrm{C}_2 + 2\mathrm{H}_2\mathrm{O} = Ti_3\mathrm{C}_2\left(OH\right)_2 + \mathrm{H}_2 \quad (2)$$

$$Ti_3\mathrm{C}_2 + 2\mathrm{HF} = Ti_3\mathrm{C}_2\mathrm{F}_2 + \mathrm{H}_2 \quad (3)$$

Reaction (2) and (3) gives rise to the surface terminations like -O, -OH, -F etc., respectively [17, 24]. MXenes have three possible structures with different layers of stacking as shown in **Figure 2(b)**, [22] The tentative elements of MXene precursor in the periodic table predicted till now presented in **Figure 2(c)** [23].

The timeline of synthesis of MXene in different year is given in **Figure 3(a)**. [25] Choice of synthesis and processing method including precursors etchant, intercalant, reaction sonication time etc. strongly influence the properties of resultant MXene. Mild alkali etchants like NaOH [26] and $NaBF_4$ [27] were also proposed to synthesis Ti_3C_2 by high temperature hydrothermal etching of Al layer from Ti_3AlC_2. This method extended to other MXenes such as Nb_2C [27]. Similarly, molten $ZnCl_2$ were

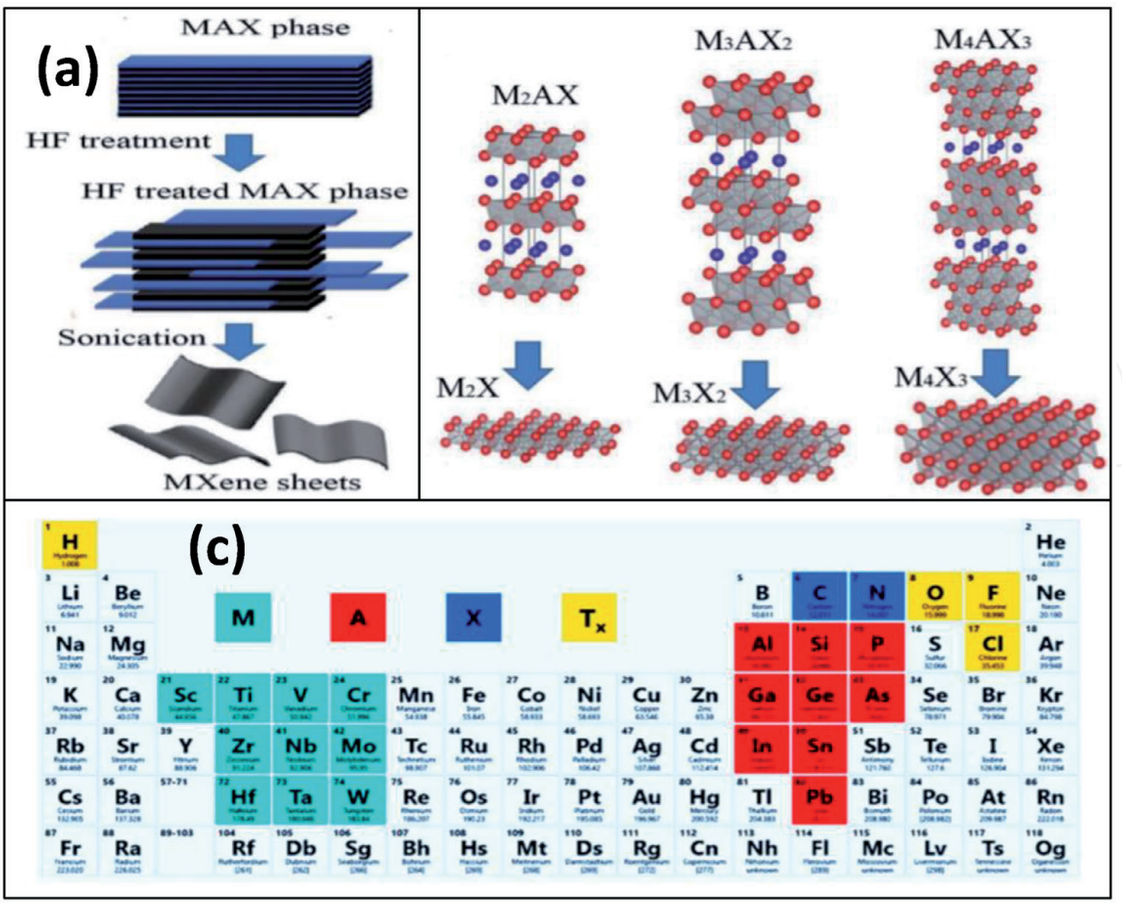

Figure 2.
(a) Schematic showing the synthesis of MXene from MAX by HF treatment, (b) synthesis mechanism of different order of MXenes by MAX phases. [22] and (c) compositions of MXene elements in periodic table (Reprinted from [23]with permission from, copyright@2020, MDPI).

used for different MAX phases like Ti_3AlC_2, Ti_2ZnN, Ti_2AlC and V_2AlC to substitute Zn^{2+} ions [28]. Another report suggested a fluoride free-electrochemical etching at room temperature synthesis of Ti_2C and Ti_3C_2 in dilute HCl [29] and NH_4Cl/TMAOH [30]. Also, a naturally delaminated MXenes with better electronic conductivity can be produced using minimally intensive layer delamination (MILD) without the use of further handshaking or sonication of MXenes [25]. More than 20 different types of MXenes have been synthesized experimentally [18]. **Figure 3(b)** represents the different etching methods that are used to synthesis different MXene products [25].

2.2 Properties

2.2.1 Electrical conductivity

MXenes have been extensively investigated by computational methods [31, 32], MXenes can be categorized into three types i.e., metallic, semi-metallic and semi-conducting [33]. Generally, bare MXenes have very high electronic conductivity with high density of states (DOS) at the fermi level. Electronic properties of MXenes are strongly influenced by the surface, morphology and stacking behavior of MXene sheets. Delaminated MXenes flakes show ultra-high electronic conductivity of upto 9880 Scm^{-1}, which can be further tuned by modifying the surface-terminations [34]. In addition to this, MXenes strongly depends on synthesis procedure which can be achieved by varying the synthesis conditions. HF etched highly defective MXene exhibits electronic conductivity of 1,000 Scm^{-1}. Whereas it improved to 4600 Scm^{-1} for powder and further enhanced to 6500 Scm^{-1} for

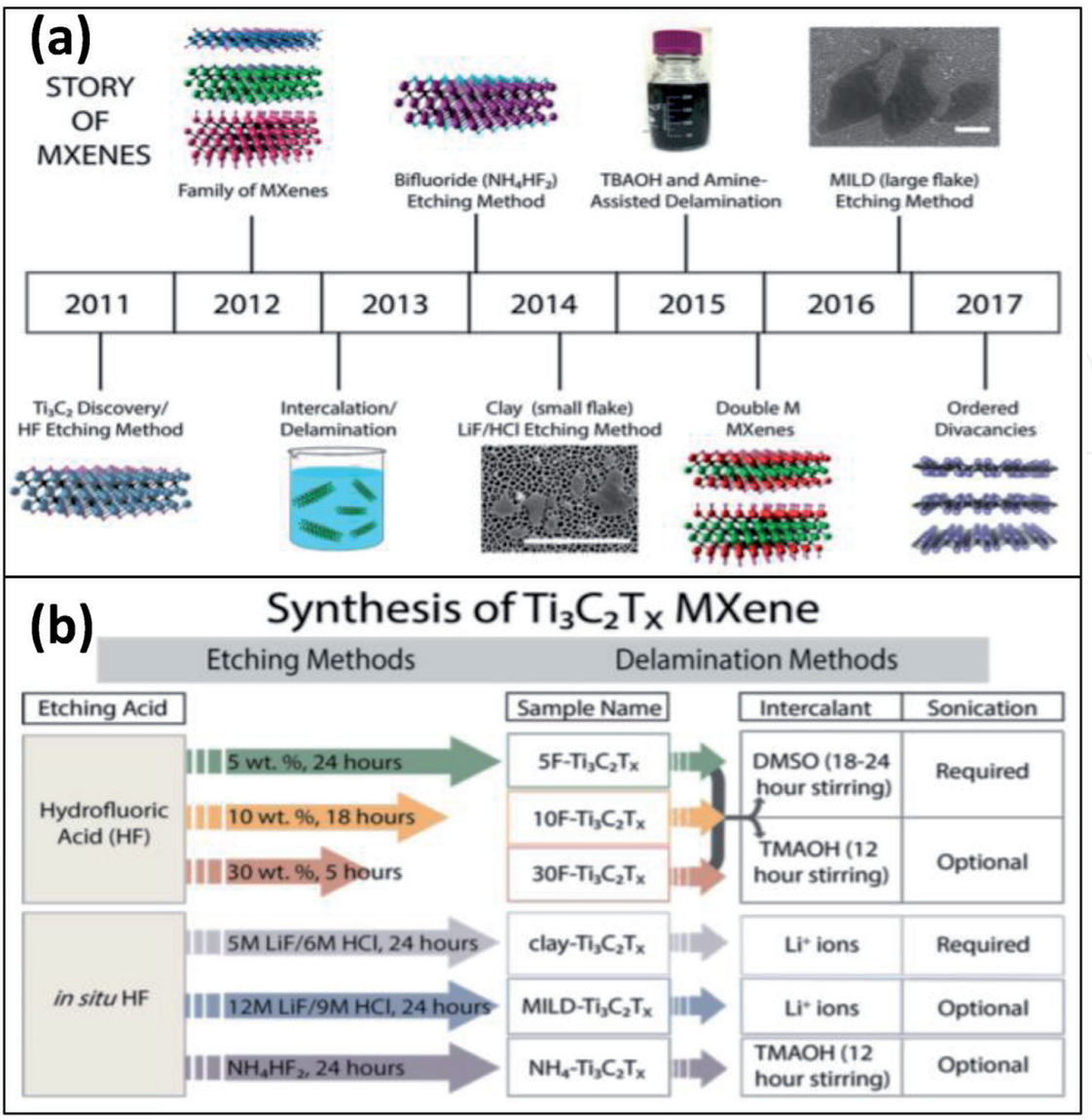

Figure 3.
(a) Timeline of synthesis of MXenes, (b) different protocols to synthesis different kind of MXenes (Source: Reprinted from [25] with permission from, copyright@2017, ACS).

delaminated MXene thick films by simply varying the etching and sonication conditions [35]. Although, Theoretical investigations shows the high electronic conductivity in MXenes. But there is still lack of knowledge and experimental expeditions to synthesize such exceptional MXene with control over surface chemistry.

2.2.2 Surface morphology

MXenes are synthesized by MAX precursors where M atoms are close packed and X atoms at interstitial sites [36]. Generally, MXenes have hexagonal close-packed structure with different order of M atoms in which M_2X follows ABABAB type order with hexagonal-stacked packing while M_3X_2 and M_4X_3 follows ABCABC type order with face-centered cubic stacking [22]. A study published by wang et al., Surface moieties play a key role in altering the properties of MXenes. The orientation and interaction between the terminal groups like -OH, -O, -F etc. strongly enhances interlayer hydrogen bonds which further improves the quality of MXenes. [37]. Also, the hydrogen bonding in MXene is highly influenced by surface terminations and interlayer spacing. Depending upon the occupancy of a functional group like -OH, -F and -O etc. the properties can be tuned for the respective application.

Intercalating the MXenes with ions, further gives a chance to mitigate the restacking behavior of MXene sheets for better performance, leading to display clay-like-behavior [38]. There is a lot to study and prepare pure MXenes for future energy applications.

2.2.3 Mechanical properties

MXenes exhibit peculiar physical and chemical properties which directly contribute to their mechanical behavior such as young's modulus, stiffness, defect generation, surface and elastic properties. Defect-rich MXenes with different terminal groups has strong covalent bonding with transition metal ion. Overall, there are various parameters which can be tunable to produce high performance MXenes. There are several theoretical studies on the mechanical, electronic as well as thermal properties of different types of MXenes [31, 39–43]. Experimentally the young's modulus of $Ti_3C_2O_2$ and Ti_3CO_2 was found to be 466 GPA and 983 GPA [44], these values were almost closer to the value predicted by theoretical simulations of 502 GPA [45]. Theoretical studies claims that M_2X exhibit much stronger in contrast to M_3X_2 and M_4X_3. But there is no experimental evidence to prove. However, in a study [46], A 5 μm thick paper film of $Ti_3C_2T_x$/PVA composite was able to hold~15,000 times its weight, which is evident to its strong wear and tear resistance property. Based on the surface terminations, there is a chance to modify surface properties of MXenes. Further investigations are needed to tune and enhance its nature.

3. Micro-fabrication techniques

3.1 Photolithography

Photolithography is a most promising technique at industrial scale which enables on-chip fabrication of high-resolution interdigital patterns of microelectrochemical systems (MEMS), Integrated Circuits (ICs), and complementary metal-oxide-semiconductors (CMOS) devices on various substrates with the help of computer-generated photomasks and photoresist designs. Recently, Jiang *et al*. fabricated all MXene based microsupercapacitors (MSCs) by spray coating on O_2 plasma treated predefined photoresists patterns prepared by direct photolithography on silicon substrates [47]. The thickness of the MXene coating was varied to get superior electrical conductivity. Device showed an ultra-high scan rate stability upto 300 V/s. Similarly, Kim and group fabricated a high performance MXene/CNT based hybrid on-chip MSCs by using Focused-ion beam (FIB) lithography technique [48]. They were able to fabricate the sub~500 nm gap between the fingers (W_g) reducing the active electrode foot print (W_e) of the device. Increasing the ratio, W_e/W_g by decreasing the gap between the electrode, which further shortens the ohmic losses. Hence improves the on-chip MXene based areal capacitance upto 317 $mFcm^{-2}$ at 50 mVs^{-1}. The capacitance retention of 32.8% was achieved even at higher scan rate of 100 Vs^{-1}. Due to imperfect resolution and ultra-narrow interelectrode gap. There are potential risks of degradation and a short circuit between the electrodes [49]. But, due to lack of electrode materials and stability issues, photo-lithography is not been used at its threshold. Xue and co-workers successfully demonstrated the electrophoretic deposition (EPD) of MXenes on the pre-patterned current collector in acetone solvent. EPD method is also grabbing attention in the scientific community [50]. There is a big room to do research. Since, photolithography technique comes out to be a challenging yet rewarding in terms of industrial fabrication and scalability for micro-supercapacitor applications.

3.2 Inkjet printing

Inkjet printing is a very popular technique for fabricating MSCs with excellent precision of designed pattern on various non conducting substrates. Nowadays, inkjet printing is gaining momentum in the scientific community. One can get desired thickness of printed layer to meet the certain applications. As name suggests inkjet printing is solely depends upon the prepared liquid ink.

There are three basic parameters which defines the behavior of the liquid inks:

1. Reynolds No. (R_e)

$$R_e = \frac{v\rho_a}{\eta}$$

2. Weber (W_e)

$$W_e = \frac{v^2\rho_a}{\gamma}$$

3. Ohnesorge (O_h)

$$O_h = \frac{\sqrt{We}}{Re.}$$

Where ρ is the density (Kg/m^3), η is the dynamic viscosity ($N.S/m^2$), γ is the surface tension (N/m), v is the velocity (m/s), a is the nozzle diameter (m) [5]. To generate, stable ink droplets, numerical simulations have demonstrated that the rheology behavior of the ink should be in the range of $1 < Z < 10$ for better results. Also, to predict the rheological characteristics of a drop of ink, the inverse Ohnesorge number Z is used i.e., $Z = 1/O_h$. [51]. As increase in demand of self-charged and wearable devices,highly functionalized conductive$Ti_3C_2T_x$ (MXene) has attracted attention to directly prepare a highly stable conductive ink in various organic solvents. Inkjet printing is the cheapest and most viable technique to fabricate MXene based MSCs. Recently, Zhang et al. fabricated additive-free MXene ink based MSCs on flexible substrate shown in **Figure 4(a)**, N-Methyl-2-pyrrolidone (NMP) based MXene ink shows excellent volumetric capacitance of 562 F/cm^3 by inkjet printing. Demonstrating stable ink formulation in different organic solvents displayed in **Figure 4(b)**. The extrusion printed patterns exhibits power density as high as 11.4 μWcm^{-2}. Also, by adjusting the printing pass, the authors were able to reduce the sheet resistance upto 35 Ω/sq. from 445 Ω/sq. the areal capacitance and cycling stability of inkjet and extrusion printed MSC is given in **Figure 4(c,d)**. This study opens a new technique to fabricate low cost MXene ink-based MSC devices [52]. MXene aqueous ink with excellent oxidation resistance power were directly printed on paper substrate. The hybrid MXene suspension capped with sodium ascorbate (SA) displays the superior stability of upto 20 days. Due to its oxidation resistance nature and large interlayer spacing the conductivity of SA MXene improves to 119 Scm^{-1} this shows that there is still big room to develop MXene ink based printable devices for MSC Application [53].

3.3 Laser scribing

Laser engraving is another emerging cost-effective technique for the fabrication of MSCs on various customized substrates. Precise resolution with fast scanning speed makes this technique a superior approach in the field. But with all above benefits, there are few difficulties faced during the optimization of wavelength,

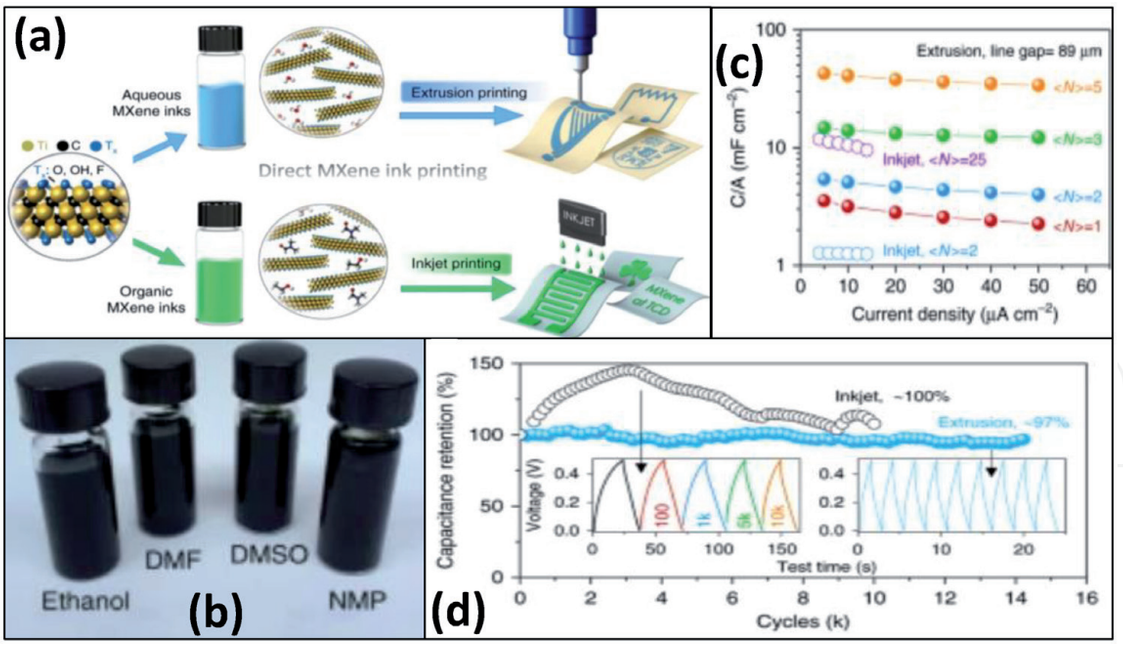

Figure 4.
(a) Schematic of direct printing of aqueous MXene inks used for extrusion printing and organic MXene inks used for inkjet printing on various substrates, (b) plot showing the areal capacitance of inkjet and extrusion printed MSC with various printing passes <N > = 2 and 25, (c) picture of different MXene organic inks, (d) cycling stability of inkjet and extrusion at current densities of 14 and 200μAcm^{-2}. (Source: Reprinted from[52], permission from, copyright @2019, Nature).

resolution and accurate speed suitable for the fabrication of MSCs on different substrates. Tang and co-group demonstrated the direct laser writing of $Ti_3C_2T_x$ interdigital electrodes by tuning the direction of laser scanning and rate. Interlayer spacing of restacked MXene was increased due to high photothermal oxidation effect of direct laser writing which enhanced the ion transport nature of the films [54]. Wang et al., fabricated double sided flexible asymmetric MSCs on thin nickel sheet by using spray coating technique followed by cutting of interdigital patterns by UV laser. By increasing the mass of active material, the maximum capacitance improved to 34 mF cm^{-2} approximately double as compared to the previous one. The fabricated double-sided device displayed considerable energy density of 2.62 μWhcm^{-2} at 2 mA cm^{-2} [55]. Further, Kurra and co-members reported a high areal capacitance based on clay-like MXene MSCs fabricated directly on paper by using a CO_2 laser. Clay-like MXene shows superior power density of 46.6 mWcm^{-2} at energy density of 0.77 μWhcm^{-2}, opening a new method to fabricate on-paper MSC devices [56].

3.4 Screen printing

Screen printing technology is one of the popular traditional technique to transfer predesigned ink patterns of active materials on various substrates. Important features of this technique are its scalability, reproducibility and repeatability. The screen printing technique is simple with high efficiency unlike other printing techniques, showing the enormous opportunity to explore. This inexpensive method can be used manually or even by automated machines. Generally, the setup includes the mesh screen with little gap between the substrate. With the help of squeegee, the ink is flooded over the screen mesh to print on the substrate [57]. Screen printing gained considerable attention to directly print MXene ink-based electrodes directly on a target substrate. Screen printing solely depends on rheological properties of ink which should be highly viscos and show a good shear thinning behavior. Additionally, the size and resolution of electrodes depends on mesh size. Recently,

screen printed MSCs were fabricated on paper by using homogeneous ink of MXene sediments. The perfectly tuned thickness of MSCs reduced the sheet resistance upto 2.2 Ω sq^{-1} and gives excellent electrical conductivity of upto 450 Scm^{-1}. The energy density reached to 158 $mFcm^{-2}$ which is highest of its kind [58]. A two-step screen printing technique is employed to fabricate asymmetric MSC with interdigital pattern on paper as well as PET substrate. High energy density of 8.8μ$Whcm^{-2}$ in PVA-KOH was observed, far superior than many of other reports [59]. There are advantages of the technique to get high mechanical stability on different substrates which definitely enhances the electronic conductivity of the fabricated devices.

3.5 3D printing

3D printing technology has attracted lot of attention for scalable fabrication of 3D architectures for the development of small and portable electronics. Recently a new trend has been introduced to fabricate 3D MSCs. This method is less complex and easy to handle compared to other lithography techniques. MXenes are the emerging material to be introduced by this technique for the fabrication of gel-type ink-based 3D MSC device to enhance its areal and volumetric capacitance. Recently, Orangi et al., fabricated an ultra-stable gel-type MXene ink based MSC given in **Figure 5(a)** by modifying its viscoelastic behavior in universal water solvent. The as fabricated device **Figure 5(b)** displays a maximum energy density of 51.7μ$Whcm^{-2}$. Further optimizations of active material layer have been done to further enhance the areal capacitance. Good adhesion & no change of electrochemical performance, even on applying stress and strain on the device given in **Figure 5(c, f)**. The cyclic voltametric curves of all MSCFs and the best performing MSCF-10 as shown in **Figure 5(d, e)** [60]. Similarly, Free standing $Ti_3C_2T_x$ (MXene) ink-based 3D MSCs were fabricated followed by freeze drying for shape retention. To increase the

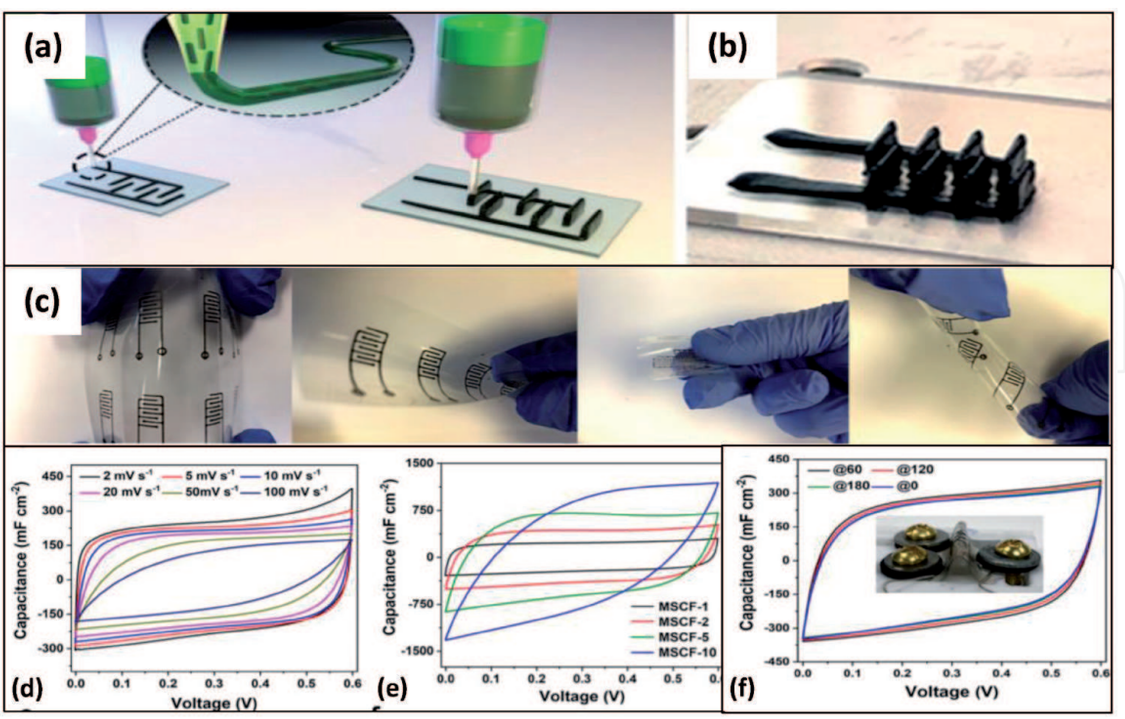

Figure 5.
(a) Demonstration of 3D interdigital MSC by 3D printing technique, (b) As printed MSC on glass substrate, (c) picture showing the strong adhesion of printed pattern on plastic substrate with great flexibility during repeated bending cycles, (d) CV curves of MSCF-1 at different scan rates from 2mVs^{-1} to 100 mVs^{-1}, (e) CV curves of various MSCFs at scan rate of 5 mVs^{-1}, (f) CV curves of MSCF-10 at scan rate of 10 mVs^{-1} at different bending angles (Source: Reprinted from [60] with permission from, copyright@2020, ACS).

stability and electrical conductivity, optimizing the mass loading to get the better viscoelastic behavior are the key parameters to obtain high areal capacitance. The maximum areal capacitance of 2.1 Fcm^{-2} at 1.7 $mAcm^{-2}$ was achieved by a single MSC device. This unique technique has a wide base to explore micro-supercapacitor applications just by playing with the rheological properties of inks [61].

3.6 Other techniques

Unconventional methods have also been employed to fabricate the MXene based MSCs. A group reported the direct writing of highly concentrated MXene-in-water inks of upto 30 mg/mL in water on different substrates by using commercial roller ball pen. Interdigital electrodes were designed to fabricate Micro-supercapacitors. Areal capacitance of single MXene MSC was 5 $mFcm^{-2}$ and by joining four MSC devices in series, the potential window reached upto 2.4 V which is evident for the development of flexible MSC devices [62]. Zhang *et al.* used a novel stamping technique to fabricate interdigital MSC on various substrates by using Ti_3CNT_x (MXene) inks. They observed an areal capacitance upto 61 $mFcm^{-2}$ at 25 μAcm^{-2} which outperforms many of previous reports. The device also exhibits high coulombic efficiency of 100% even after 10,000 cycles. This novel approach opens a new exciting method to fabricate MSC in easy and facile way [63]. Hue *et al.* demonstrated a facile two-step laser jet vacuum assisted filtration approach to fabricate all-solid-state MXene based symmetric microsupercapacitors followed by gold sputtering on regular A4 paper. The device exhibits high energy density in the range of 5.48–6.1 $mWhcm^{-2}$ depending upon the deposited thickness of the electrode. The maximum areal capacitance of 27.29 $mFcm^{-2}$ was achieved. This

Techniques	Method	Merits	Demerits
Photolithography	Direct	Wafer-scale manufacturing, uniform & high-resolution patterning [47, 48].	Multi-step process, template assisted, time consuming method [48].
Inkjet and Extrusion Printing	Indirect	Scalable production, customized design, less wastage of material [52, 62].	Uncontrollable procedure of ink synthesis, Low resolution, nozzle jamming is one of the main disadvantages of this technique [52].
Laser Scribing	Direct	Cost effective, fast simple, high controllability [54, 55].	Confined to very few types of materials [6].
Screen Printing	Indirect	Highly scalable and fast process [59].	Relatively low-resolution power
3D Printing	Indirect	Controllable design of patterns, versatile thickness control [61].	Limited to few materials, complex processibility [61].
Electrophoretic Deposition	Direct	Economically viable, facile procedure [50].	Limited applicability.
Vacuum-assisted-filtration	Indirect	Easy process, controlled thickness [67].	Low resolution, size and shape limited.

Table 1.
Merits and demerits of various fabrication techniques of MSCs.

simple strategy of laser jet printed mask-assisted technique exhibits the potential for low cost fabrication method without compromising with device performance [64]. Li and co-workers proposed a simple scratch method to fabricate $Ti_3C_2T_x$/EG (MXene/exfoliated graphene) based MSC. A common syringe was employed with custom made X/Y axis instrument to fabricate the interdigital patterns. The device was able to display electrochemical stability upto 5000 charge/discharge cycles with around 90% retention of capacitance. This new approach shows promising results with almost negligible cost of fabrication at large scale [65]. Similarly, another group used automated scalpel technique to carve semi-transparent PEDOT/$Ti_3C_2T_x$ heterostructures micro-supercapacitors. Device exhibit considerably high capacitance of 2.4 $mFcm^{-2}$ at 10 mVs^{-1} shown by 100 nm device with almost 58% of capacitance retention at scan rate of 1000 mV/s. Further changes in color were observed on applying voltage 0.6 to 0 V and − 0.6 to 0 V while discharging which displays good electrochromic behavior PEDOT/$Ti_3C_2T_x$ MSCs [66]. Advantages and disadvantages of various fabrication techniques of MSCs can be seen in **Table 1**.

4. MXene and its 2D hybrids for micro-supercapacitors

4.1 MXene based materials

In the past few years, MXenes have shown promising results for micro-supercapacitor applications. Due to their unique morphology, high metallic conductivity~10,000 Scm^{-1} and excellent intercalation behavior. Kurra *et al.* reported all MXene based low cost and highly scalable coplanar microsupercapacitors on paper substrates, the clay like MXenes based MSC displays the electrical conductivity of 128 Scm^{-1} and areal capacitance of 25 $mFcm^{-2}$ in PVA-H_2SO_4 gel electrolyte. This study suggests the thickness of the active material plays a key role in the enhancement of the areal capacitance [56]. Similarly, Jiang and co-workers reported a wafer scale approach to fabricate an on-chip MXene based MSC device. The typical procedure includes photolithography of interdigital patterns followed by spray coating. The optimized $Ti_3C_2T_x$ – 0.3 μm exhibits more capacitive behavior. The fabricated device was able to convert constant output positive peak voltage of 0.6 V into-0.56 V which is comparable with commercially available capacitor (4mF). Demonstrating the advancements of MXene based MSCs for better alternative than bulky electrolytic capacitors in circuits [47]. Peng *et al.* fabricated interdigital patterned device by spray coating of $Ti_3C_2T_x$ flakes directly on glass substrates which shows considerable areal capacitance of 19.6 $mFcm^{-2}$ at 20 mVs^{-1} with ultra-high volumetric capacitance of 356.8 Fcm^{-3} at 0.2 $mAcm^{-2}$ which is better than many of the carbon materials reported in the literature. But, the significant increase of areal capacitance 27.3 $mFcm^{-2}$ at 20 mVs^{-1} can be seen by introducing the platinum current collectors [68]. Recently, A new strategy has been employed to pattern semi-transparent film of MXene based hybrid device on glass substrate without using any mask. An automated scalpel tool was used to produce micropatterns at various levels of transparency. On the increase of transparency from 38–88%, areal capacitance from 19 to 283 μFcm^{-2} can be evidently seen to be increased because of thick layers of MXenes. In contrast, With the increase of coating cycle, the resistance also increases from 0.8 to 2 kΩ. The device demonstrated excellent capacitive behavior, offers variety of tunable approach by which one can enhance its physiochemical properties [69]. Li et al., reported the fabrication of a double sided MSCs (DSMSCs) based on MXene ink with high working potential window of 7.2 V connected in different series and parallel configurations. With the decrease of interspace between MXene electrodes, the steep rise of capacitance can be seen.

Hence, DSMSC with 10 μm interelectrode gap displays the highest volumetric capacitance of 308 Fcm^{-3} at 5 mVs^{-1} with ultra-high coulombic efficiency of 96.4% even after 10,000 cycles [70]. Quain and group reported direct writing with pen using additive-free MXene ink on flexible paper and non-paper substrates. The ink suspension displays good polydispersity index of 0.549 which consists of both small and large flakes of MXene at 30 mg mL^{-1} This single step fabrication technique is used to write on various flexible substrates. High potential window upto 2.4 V was also achieved by connecting four MSCs in series [62]. A facile Freeze-and -Thaw-assisted method (FAT) was used to produce two-atom thin layers of MXene with extra ordinary strength and flexibility. FAT-MXene exhibits an Areal capacitance of 23.6 $mFcm^{-2}$ with high volumetric capacitance. 591 Fcm-3 at 20 mVs^{-1} [71]. Zhang and group-fabricated a flexible asymmetric microsupercapacitors comprising MXene and MXene-MoO_2 films as negative and positive electrodes. The fabrication process includes vacuum filtration of the films followed by laser cutting of the interdigital patterns as given in the schematic **Figure 6(a)**. The asymmetric device exhibits large potential window of 1.2 V which is almost double of symmetric device. The device delivers volumetric capacitance of 63.3 Fcm^{-3} and the CV and GCD curves shown in **Figure 6(b, c)** with excellent capacitance retention of 88% after 10,000 cycles **Figure 6(d)** [72]. Huang *et al.* reported a facile strategy to produce free standing-thick MXene sheets by vacuum filtration. The films exhibit an ultra-high conductivity upto 1.25 × 10^5 Sm^{-1} for flexible-MSC. Further efforts has been done to fabricate an interdigital patterned MSC device which displays an considerable areal capacitance of 340 $mFcm^{-2}$ with volumetric capacitance of 183 Fcm^{-3} and the corresponding energy density and power density are 12.4 $mWhcm^{-3}$ and 218 $mWcm^{-3}$ [73]. Another group demonstrated a highly conductive paper based MXene electrodes possessing a reasonable areal capacitance of 23.4 $mFcm^{-2}$ at 0.05 $mAcm^{-2}$. One step process fabrication of electrodes in series as well as parallel to further get the desired capacitance [74].

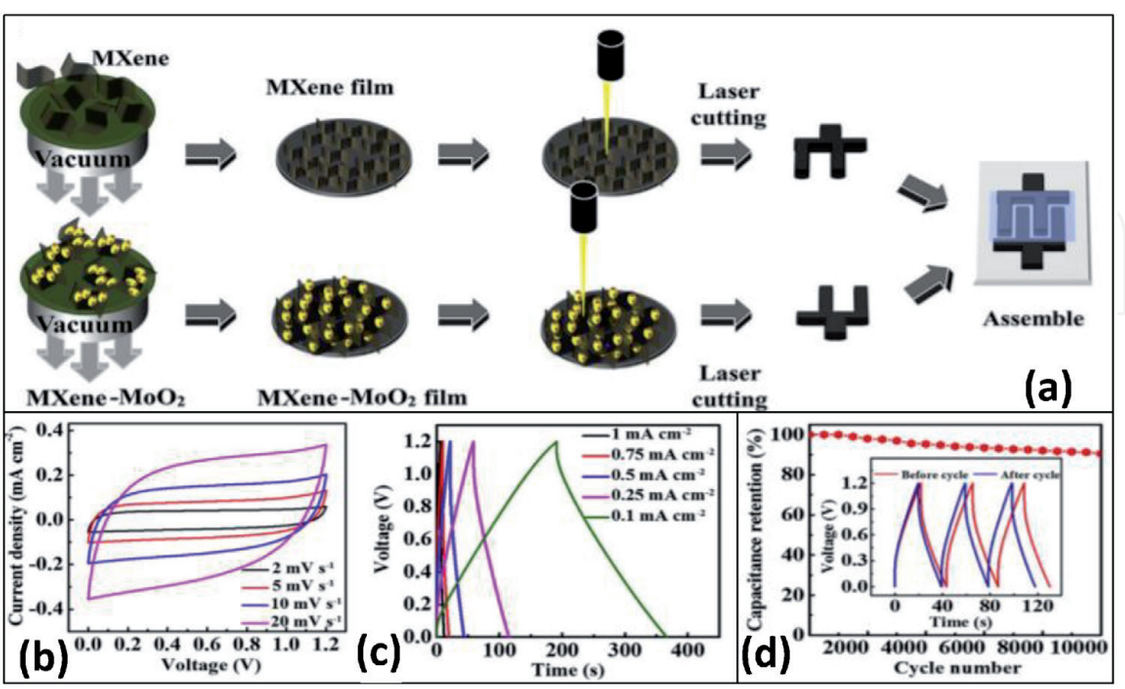

Figure 6.
(a) Fabrication procedure of MXene//MXene-MoO_2-AMSCs asymmetric MSC, (b) cyclic voltametric curves at different scan rates from 2 to 20 mVs^{-1}, (c) Galvanostatic charge–discharge at different current densities from 0.1 to 1$mAcm^{-2}$, (d) cyclic stability at current density of 0.5 $mAcm^{-2}$. Inset shows the charge–discharge cycles after and before10,000 cycles (source: Reprinted from [72] permission with Elsevier).

4.2 MXene and carbon materials

Recently, Kim et al., reported a scalable production of MXene/CNT based MSCs with a 500 nm gap between the interdigital fingers exhibiting fast ion diffusion for superior conductivity. High areal capacitance of 317.3 $mFcm^{-2}$ was achieved at 50 mVs^{-1} by composite of S-DWCNT/MXene in PVA-H_2SO_4 gel electrolyte. It is also observed that by decreasing the electrodes gap 10 μm to 500 nm, improves the ionic transfer rate, leading to increase in areal capacitance and energy density [48]. A 3D MXene/rGO self-healable aerogel MSC were reported by Yue and group. The fabrication process is shown in **Figure 7(a, b)** They employed new approach to fabricate highly stable device by keeping in focus to real time applications. Fabricated device was encapsulated into self-healing Polyurethane (PU) which enabled the device to adhere the external damage. The composite aerogel exhibited an exceptional recovery of electronic and mechanical properties even

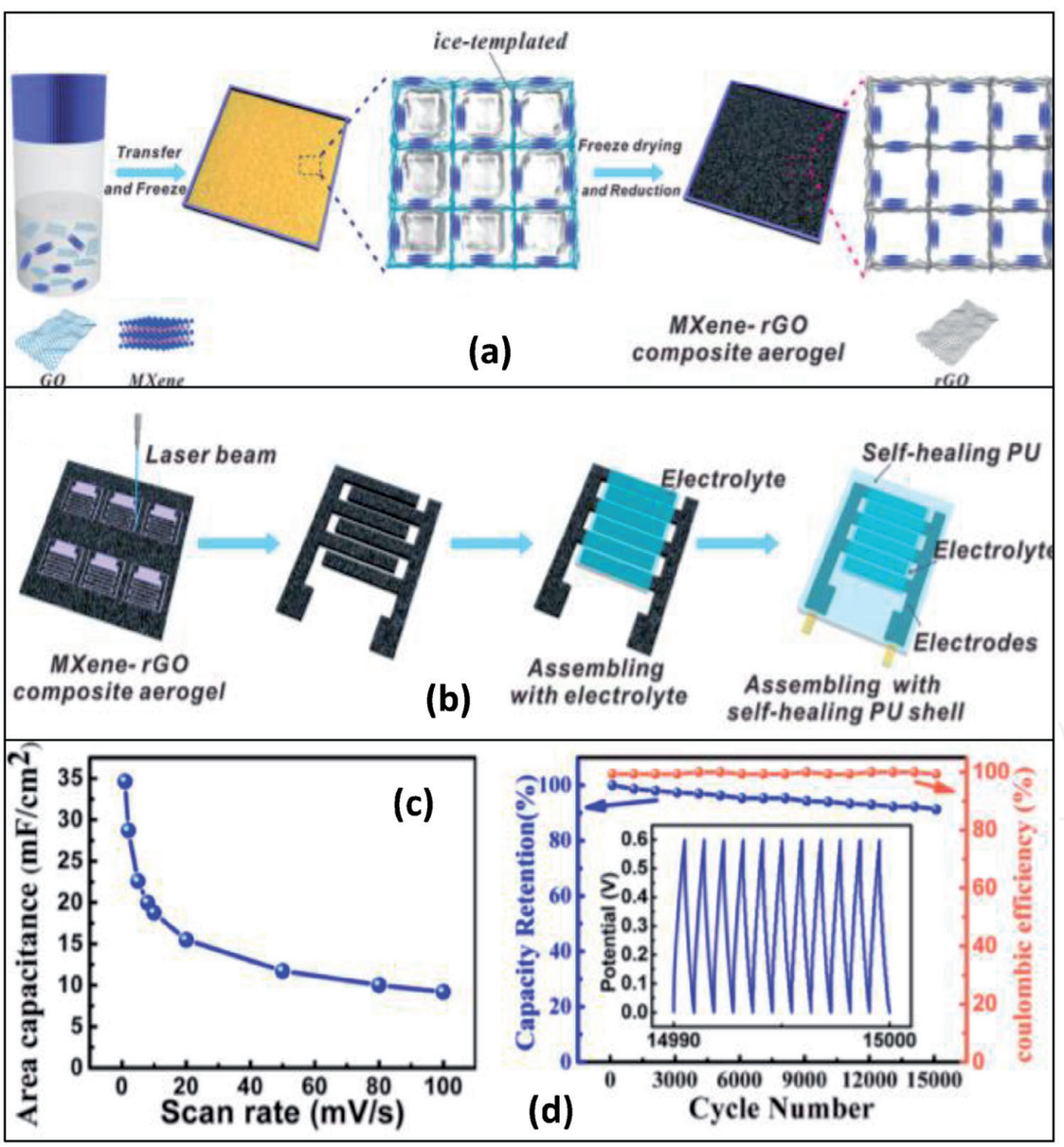

Figure 7.
(a) Fabrication procedure of MXene-rGO composite aerogels, (b) laser cutting of interdigital pattern on MXene-rGO composite followed by assembling with self-healing PU, (c) graph showing the areal capacitance vs. scan rate MXene-rGO composite, (d) cycling stability of MXene-rGO composite aerogel MSC at 2 $mAcm^{-2}$ (inset showing the GCD curves from 14990th to 15000th cycles (source: Reprinted from [75] with permission from, copyright@2018, ACS).

after full breakdown and shows the areal capacitance of 34.6 mF cm^{-2} at 1 mVs^{-1}, the areal capacitance and Cycling stability is shown in **Figure 7(c, d)**. [75] Couly *et al.* fabricated a high performing asymmetric flexible micro-supercapacitor based on MXene as negative and rGO as positive in both sandwich as well as interdigital configurations by using simple spray-coating of active material on PET substrates. The working potential window increased to 1 V for asymmetric device even with no. of bending and folding cycles, the maximum areal capacitance of 2.4 $mFcm^{-2}$ at 2 mV/s was achieved. This study shows MXene as a promising material for negative electrode in asymmetric configuration with good stability and robust performance [76]. There is still wide room for further exploitation of carbon-based materials for micro-supercapacitor applications. A new emerging trend to produce nanofibers based on yarn type super capacitors for self-charged and wearable energy storage devices. MXenes have shown great potential to produce textile-based energy storage devices due to its robust stability as well as extraordinarily tunable properties. Yu and group, reported a helical shape MXene/CNT scaffold hybrid structure with reasonable volumetric capacitance of 19.1 Fcm^{-3} at 1.0 Acm^{-3} in 6 M of aqueous LiCl electrolyte. The MXene/CNT fiber exhibit good Energy density of 2.55 to 1.15 $mWhcm^{-3}$ at power density of 0.046 to 1.82 W cm^{-3} in LiCl gel electrolyte. The best performing device displays the capacitance retention of 19.5 Fcm^{-3} (84%) at current density of 1.0 Acm^{-3} [77]. MXene/rGO hybrid fiber supercapacitors were fabricated by wet-spinning assembly strategy with extremely high volumetric capacitance of 586.4 Fcm^{-3} at 10 mV/s. The composite fibers display an ultra-high electrical conductivity of 2.9×10^4 S cm^{-1}. They observed that the flexibility of the fiber can be increased by adjusting the concentration of graphene [78].

In another report by chen and group, MXene-MoS_2 based free standing MSCs were fabricated by simple and low-cost vacuum filtration method followed by carving of interdigital patterns with laser source. By introducing the MoS_2 into MXenes which further enhances the electrochemical performance with almost 60% increase as compared to pristine MXene. i.e., the fabricated device displays a high specific capacitance of 173.6 F/cm^3 at the scan rate of 1 mV/s, MSC shows around 98% of capacitance retention with 89% of coulombic efficiency even after 6000 cycles along with several bending angle of device upto 150°. The above study demonstrated huge potential of TMDs which can be introduced with MXenes to make high performing MSC devices [67]. Li *et al.* demonstrated a strategy to mitigate the self-restacking of MXene layers by introducing RuO_2 nanoparticles by simple wet chemical phase reaction to improve the ion exchange rate. Also integrating with conductive Ag nanowires into the MXene further decrease the surface resistance of electrodes. The optimized MSC device achieved an ultrahigh volumetric capacitance of 864.2 Fcm^{-2} at 1 mV/s with 90% of capacitance retention even after 10,000 cycles [79]. For the first time, Wang *et al.* reported PANI/MXene based film electrodes with an exceptionally high volumetric capacitance of 1167 Fcm^{-3}. The asymmetric device by taking MXene as a negative electrode exhibit a maximum energy density of 65.6 WhL^{-1} which overshadows many of the previous reported MXene based Micro-supercapacitors [80]. A new kind of stretchable micro-supercapacitors based on MXene/Bacterial Cellulose (MXene/BC) composite free-standing paper were fabricated showing an exceptionally high young's modulus of 15–35 GPa with tensile strength of upto 200–300 GPa. Here BC acts as a spacer intercalated between the MXene sheets to prevent the re-stacking of MXene flakes. A conventional laser cutting tool used to fabricate stretchable micro-supercapacitor device was prepared which displays the high areal capacitance of 111.5 mF cm^{-2} in parallel device configuration with reasonable energy density of 0.00552 $mWhcm^{-2}$ [81]. Shao *et al.* synthesized MXene-polymer composite nanofibers as flexible

yarn electrodes by simple electrospinning the active material on PET sheets. The symmetric device displays high areal capacitance of upto 18.39 $mFcm^{-2}$ at scan rate of 50 mVs^{-1} which is better than many other carbon based yarn fiber supercapacitors [82]. Another group of researchers fabricated MXene/PEDOT-PSS based yarn supercapacitors (YSCs). A 3 cm flexible fiber shows extraordinarily high length capacitance of 131.7 mF cm^{-1} at 0.2 $mAcm^{-1}$ with capacitive retention of 95% even after 10,000 cycles. They observed the reasonable contribution of conductive-polymer PEDOT-PSS in improving the device performance, suggesting a potential candidate in flexible yarn supercapacitor in portable electronics [83]. A new strategy has been employed to fabricate dual-core yarn supercapacitor (YSC), fabrication process shown in **Figure 8(a, b)** consist of rGO and MXene hybrid fibers encapsulated with PVA-H_2SO_4. The average diameter of YSC is ~500μm showing the superior linear capacitance 43.6 $mFcm^{-1}$ at 20 mVs^{-1}. The areal capacitance was maintained above 175 $mFcm^{-2}$ with respect to increasing length. They observed the charge transfer resistance (Rct) ESR of YSCs decreases gradually with increase in length such as ~30.3 Ωcm^{-1} at 3 cm, 3.9 Ωcm^{-1} at 10 cm to 1.6 Ωcm^{-1} at 15 cm the graphs are shown in **Figure 8(c, d)**. The YSC device of 15 cm displayed areal density of 54.5 $\mu Whcm^{-2}$ at a power density of

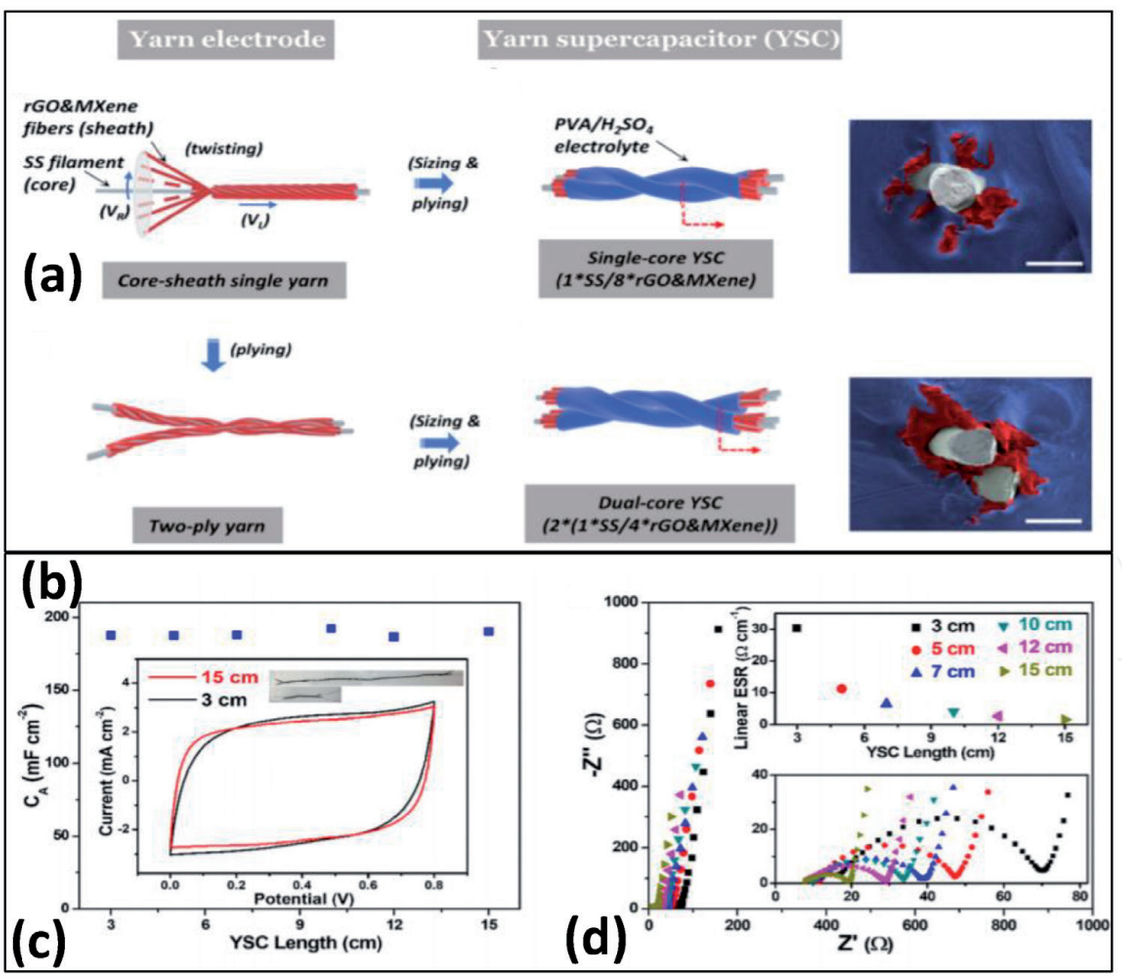

Figure 8.
*Schematic illustrations of fabrication process of (a) 1*SS/S* rGO&MXene YSC single core YSC cross-sectional SEM image (scale bar -100 μm), (b) (2*(1*SS/4*rGO&MXene)) dual-core YSC cross-sectional SEM image (scale bar -100 μm), (c) areal capacitance of dual-core YSC inset: CV curves at 20mVs^{-1} in 3 and 15 cm, (d) comparison of Nyquist plots of dual-core YSCs from 1 MHz to 0.01 Hz in different length inset: Linear ESR as a function of YSC length (top), zoom in image of Myquist plots (bottom) (source: Reprinted from [84]with permission from, copyright@2020, ACS).*

Material	Method	Electrolyte	Potential Window	Device Performance		Specific Capacitance		Capacitance Retention	References
				Energy Density	Power Density	Areal	Volumetric		
$Ti_3C_2T_x$ (100 nm-25 μm)	Photo-lithography		0 to 0.6	_____	PVA-H_3PO_4	0.5 $mFcm^{-2}$ @120 Hz	30 Fcm^{-3} @120 Hz	_____	[47]
$Ti_3C_2T_x$/CNT $_{500nm}$	FIB Lithography	PVA-H_2SO_4	0 to 0.6	_____	_____	317 $mFcm^{-2}$ @ 50mVs^{-1}	_____	_____	[48]
$Ti_3C_2T_{x\ N=25}$ $Ti_3C_2T_{x\ N=5}$	Inkjet Extrusion	PVA-H_2SO_4	0 to 0.5	_____ 0.32 $\mu Whcm^{-2}$	_____ 11.4 μWcm^{-2}	12 $mFcm^{-2}$ _____	562 Fcm^{-3} _____	100% (10,000) 97% (15,000)	[52]
SA- $Ti_3C_2T_x$ P-$Ti_3C_2T_x$	Inkjet Inkjet	PVA-H_2SO_4	0 to 1	100.2 $mWhcm^{-3}$ _____	1.9 Wcm^{-3} _____	108.1 mF cm^{-2} @1 Ag^{-1} 48.4 $mFcm^{-2}$ at 1Ag^{-1}	720.7 Fcm^{-3} @1 Ag^{-1} _____	94.7% (4,000) 72.4% (4,000)	[53]
$Ti_3C_2T_x$	Laser Writing	3 M H_2SO_4	0 to 0.6	0.25 $\mu Whcm^{-2}$	2.94 $mWcm^{-2}$	15.03 $mFcm^{-2}$	_____	105% (10,000)	[54]
Double sided Zn//MXene (Asymmetric) Carbon//MXene (Asymmetric)	Laser writing Laser writing	PVA- Zn $(CF_3SO_3)_2$ PVA-LiCl	0 to 1.1 0 to 0.8	_____ 2.62 $\mu Whcm^{-2}$	_____ _____	66.5 $mFcm^{-2}$ 52.3 $mFcm^{-2}$ @2$mAcm^{-2}$	_____ _____	86% (5,000) _____	[55]
Clay like $Ti_3C_2T_x$	Laser Writing	PVA-H_2SO_4	0 to 0.6	0.77 $\mu Whcm^{-2}$	46.6 $mWcm^{-2}$	25 $mFcm^{-2}$	_____	92% (10,000)	[56]
$Ti_3C_2T_x$ Sediments	Screen Printing	PVA-H_2SO_4	0 to 0.6	1.32 $\mu Whcm^{-2}$	778.33 μWcm^{-2}	158 $mFcm^{-2}$	_____	95.8% (16,000)	[58]
MXene//Co-Al layered double hydroxide (Asymmetric) MXene	Screen Printing Screen Printing	PVA-KOH PVA-KOH	0.4 to 1.45 0 to 0.6	8.84 $\mu Whcm^{-2}$ 3.38 $\mu Whcm^{-2}$	0.23 $mWcm^{-2}$ _____	40.0 mF cm^{-2} @0.75bmAcm^{-2} 25 $mFcm^{-2}$	_____ _____	92% (10,000) _____	[59]
$Ti_3C_2T_x$	3D Printing	PVA-H_2SO_4	0 to 0.6	8.4 $\mu Whcm^{-2}$	3.7 $mWcm^{-2}$	168.1 $mFcm^{-2}$	_____	_____	[60]

Material	Method	Electrolyte	Potential Window	Device Performance		Specific Capacitance		Capacitance Retention	References
				Energy Density	Power Density	Areal	Volumetric		
$Ti_3C_2T_x$	3D Printing	PVA-H_2SO_4	0 to 0.6	0.0244 $mWhcm^{-2}$	0.64 $mWcm^{-2}$ @ 4.3 $mAcm^{-2}$	2.1 Fcm^{-2} @1.7 $mAcm^{-2}$	_____	90% (10,000)	[61]
$Ti_3C_2T_x$	Direct Writing	PVA-H_2SO_4	0 to 0.6	_____	_____	5$mFcm^{-2}$	_____	_____	[62]
l-$Ti_3C_2T_x$	Stamping Strategy	PVA-H_2SO_4	0 to 0.6	0.63 $\mu Whcm^{-2}$	0.33 $mWcm^{-2}$	56.8 $mFcm^{-2}$ @ 10mVs^{-1}	_____	93.7% (10,000)	[63]
$Ti_3C_2T_x$	Laser jet Printing	PVA-H_2SO_4	0 to 0.6	6.1 $mWhcm^{-3}$	_____	27.29 $mFcm^{-2}$ @0.25 $mAcm^{-2}$	_____	_____	[64]
$Ti_3C_2T_x$	Scratch method	PVA-H_3PO_4	0 to 0.7	2.3 $mWhcm^{-3}$	159.6 $mWcm^{-3}$	25.5 $mFcm^{-2}$ @ 5mVs^{-1}	_____	90% (5,000)	[65]
PEDOT/$Ti_3C_2T_X$ 100nm	Spray Coating	PVA-H_2SO_4	0 to 0.6	_____	_____	2.4 $mFcm^{-2}$ @ 10mVs^{-1}	_____	_____	[66]
Free-standing $Ti_3C_2T_x$ – MoS_2	Laser Engraving	Gelatin-$ZnSO_4$	0 to 0.8	15.5 $mWhcm^{-3}$	0.97 Wcm^{-3}	_____	173.6 Fcm^{-3} @1mVs^{-1}	98% (6,000)	[67]
s-Ti_3C_2Tx	Spray coating + Laser engraving	PVA-H_2SO_4	0 to 0.6	11–18 $mWhcm^{-3}$	0.7–15 W cm^{-3}	27.3 $mFcm^{-2}$ @ 20mVs^{-1}	356.8 Fcm^{-3} @ 0.2 $mAcm^{-2}$	100% (10,000)	[68]
90 nm $Ti_3C_2T_x$ thin film	Dip Coating + Automated Scalpel patterning	PVA-H_3PO_4	0 to 0.6	_____	_____	_____	1500 Fcm^{-3}	_____	[69]
$Ti_3C_2T_X$-MSC 10 μm	Laser Etched	PVA-H_2SO_4	0 to 0.6	_____	_____	_____	308 Fcm^{-3} @5mVs^{-1}	93% (10,000)	[70]
$Ti_3C_2T_X$	Mask-assisted vacuum filtration	PVA-H_2SO_4	0 to 0.6	10.3 to 29.6 $mWhcm^{-3}$	18.6 to 3.1 Wcm^{-3}	23.6 $mFcm^{-2}$	591 Fcm^{-3}	97.8% (2,000)	[71]

Material	Method	Electrolyte	Potential Window	Device Performance		Specific Capacitance		Capacitance Retention	References
				Energy Density	Power Density	Areal	Volumetric		
$Ti_3C_2T_X$ // $Ti_3C_2T_X$-MoO_2-AMSCs (Asymmetric)	Vacuum filtration + Laser cutting	PVA- LiCl	0 to 1.2	9.7 $mWhcm^{-3}$	0.198 Wcm^{-3}	~19 $mFcm^{-2}$	63 Fcm^{-3} @ 2mVs^{-1}	88% (10,000)	[72]
$Ti_3C_2T_X$	Vacuum filtration + Laser cutting	PVA-H_2SO_4	0 to 0.7	43.5 $mWhcm^{-2}$ 12.4 $mWhcm^{-3}$	87.5$mWcm^{-2}$ 218.8 $mWcm^{-3}$	73–340 $mFcm^{-2}$	183–162 Fcm^{-3}	82.5% (5,000)	[73]
$Ti_3C_2T_X$ on paper	Spray coating + Laser coating	PVA-H_2SO_4	0 to 0.6	1.48 $mWhcm^{-3}$	189.9 $mWcm^{-3}$	23.4 $mFcm^{-2}$ @0.05 $mAcm^{-2}$	_____	92.4% (5,000)	[74]
$Ti_3C_2T_X$ -Graphene aerogel	Laser cutting	PVA-H_2SO_4	0 to 0.6	_____	_____	34.6 $mFcm^{-2}$ @ 1 mVs^{-1}	_____	91% (15,000)	[75]
$Ti_3C_2T_X$//rGO (Asymmetric)	Spray coating	PVA- H_2SO_4	0 to 1	8.6 $mWhcm^{-3}$	0.2 Wcm^{-3}	2.4 $mFcm^{-2}$ @2 mVs^{-1}	80 Fcm^{-3}	97% (10,000) - Interdigital	[76]
$Ti_3C_2T_X$/CNT (YSC)	_____	PVA-LiCl	0 to 0.9	2.55$mWhcm^{-3}$	45.9 $mWcm^{-3}$	_____	22.7 Fcm^{-3} @ 0.1 Acm^{-3}	99% (1,600)	[77]
$Ti_3C_2T_X$/rGO	_____	PVA-H_3PO_4	0 to 0.8	13.03 $mWhcm^{-3}$	0.59 Wcm^{-3}	_____	586.4 Fcm^{-3} @ 10 mVs^{-1}	_____	[78]
RuO_2/$Ti_3C_2T_X$	Screen printing	PVA-KOH	0 to 0.6	13.5 $mWcm^{-3}$	48.5 Wcm^{-3}	_____	864.2 Fcm^{-3} @ 1mVs^{-1}	90% (10,000)	[79]
PANI/MXene// MXene	_____	1 M H_2SO_4	0 to 1.4	65.6 WhL^{-1}	1687.3 WL^{-1}	_____	231.4 Fcm^{-3} @ 10mVs^{-1}	87.5% (5,000)	[80]
MXene/Bacterial Cellulose	Vacuum filtration + Laser cutting	PVA-H_2SO_4	0 to 0.6	0.0055 $mWhcm^{-2}$	_____	112.2 $mFcm^{-2}$	_____	_____	[81]
Polyester @MXene	Electrospinning of fibers	PVA-H_2SO_4	0 to 0.6	0.38–0.67 $\mu Whcm^{-2}$	0.09–0.39 $mWcm^{-2}$	7.99 $mFcm^{-2}$ – 18.39 $mFcm^{-2}$	~4.5 Fcm^{-3} @5 mVs^{-1}	98.2% (6,000)	[82]

Material	Method	Electrolyte	Potential Window	Device Performance		Specific Capacitance		Capacitance Retention	References
				Energy Density	Power Density	Areal	Volumetric		
MXene/ PEDOT-PSS	Fiber coating	Conductive binder PEDOT-PSS	0 to 0.5	_____	_____	131.7 $mFcm^{-1}$ @0.2 $mAcm^{-1}$	_____	90% (10,000)	[83]
rGO/MXene Hybrid	Wet-spinning	PVA-H_2SO_4	0 to 0.8	5.5 $\mu Whcm^{-1}$	510.9 μWcm^{-1} 2502.6 μWcm^{-2}	77 $mFcm^{-1}$ 377.3 $mFcm^{-2}$	23.2 Fcm^{-3}	82% (10,000)	[84]

Table 2.
Summary of recently reported MXene based micro-supercapacitors.

1251.5 μWcm^{-2} which directly outperforms the previous reported literatures [84]. The detailed summary of data is presented in the **Table 2**.

5. Future perspective and outlook

Since the discovery of MXenes in 2011 by Naguib et al. [17] MXenes have become a best choice for micro-electrodes to develop on-chip and self-charged MSC for wireless and wearable electronics applications. There is a significant increase in research on MXene based MSC due to its extraordinarily high electronic conductivity, good volumetric capacitance and excellent advancement in properties.

But, the development of MXene based MSC are still in early stage with necessity of optimization of electrode material, suitable electrolyte, substrates and many more. Right now, the focal point of researchers is on the enhancement of areal capacitance and power density of the fabricated MXene based MSC devices. However, there is an act of negligence over its property to self-discharged in open-circuit which needs to be resolved as soon as possible. One solution to this is to further integrate MSCs device with energy harvester like micro-piezoelectric or solar power cell component which will improve long term charge-storage property instead of self-discharging.

Also, the choice of electrolyte plays an important role to enhance the electrochemical performance of MSC device. Generally, polymer gel electrolyte. Particularly, PVA-H_2SO_4 is widely used ion exchange for MXene based electrodes for micro-devices. But due to low voltage window there is a call for an alternative which can help to increase the stability and voltage window. So that, there is an urgent requirement to study different electrolytes and polymers to achieve better performing MSC. In contrast to polymer matrix electrolyte, a new emerging class of quasi-solid electrolyte called as ionogel which is more mechanically and thermally stable than the regular gel electrolyte. All this demonstrates the possibility of ionogel to be a potential candidate for MSCs. To further expand potential window there is a requirement to make asymmetric devices which can further increase the voltage range above 3 V for real time applications.

Despite recent developments of $Ti_3C_2Ti_x$ (MXene) based MSCs. There is still a big room to synthesis new MXene materials and explore their properties for the better understanding of charge storage mechanism which later can pave the way for future MSCs devices.

Acknowledgements

This work was financially supported by the Department of Science and Technology (DST)-SERB Early Career Research project (Grant No. ECR/2017/001850), DST-Nanomission (DST/NM/NT/2019/205(G), DST/TDT/SHRI-34/2018), Karnataka Science and Technology Promotion Society (KSTePS/VGST-RGS-F/2018-19/GRD NO. 829/315).

Conflict of interest

The authors declare no conflict of interest.

IntechOpen

Author details

Aditya Sharma and Chandra Sekhar Rout*
Centre for Nano and Material Sciences, Jain University, Bangalore, India

*Address all correspondence to: r.chandrasekhar@jainuniversity.ac.in

IntechOpen

References

[1] Wang J, Li F, Zhu F, Schmidt OG. Recent Progress in Micro-Supercapacitor Design, Integration, and Functionalization. Small Methods. 2019;3(8):1800367.

[2] Beidaghi M, Gogotsi Y. Capacitive energy storage in micro-scale devices: recent advances in design and fabrication of micro-supercapacitors. Energy Environ Sci. 2014 Feb 20;7(3):867-84.

[3] Michael J, Qifeng Z, Danling W. Titanium carbide MXene: Synthesis, electrical and optical properties and their applications in sensors and energy storage devices: Nanomaterials Nanotechnology. 2019 Jan 17;9;1847980418824470.

[4] Bu F, Zhou W, Xu Y, Du Y, Guan C, Huang W. Recent developments of advanced micro-supercapacitors: design, fabrication and applications. Npj Flex Electron. 2020 Nov 16;4(1):1-16.

[5] Jiang Q, Lei Y, Liang H, Xi K, Xia C, Alshareef HN. Review of MXene electrochemical microsupercapacitors. Energy Storage Mater. 2020 May 1;27: 78-95.

[6] Zhang P, Wang F, Yu M, Zhuang X, Feng X. Two-dimensional materials for miniaturized energy storage devices: from individual devices to smart integrated systems. Chem Soc Rev. 2018 Oct 1;47(19):7426-51.

[7] Pech D, Brunet M, Taberna P-L, Simon P, Fabre N, Mesnilgrente F, et al. Elaboration of a microstructured inkjet-printed carbon electrochemical capacitor. J Power Sources. 2010 Feb 15;195(4):1266-9.

[8] Chmiola J, Largeot C, Taberna P-L, Simon P, Gogotsi Y. Monolithic Carbide-Derived Carbon Films for Micro-Supercapacitors. Science. 2010 Apr 23;328(5977):480-3.

[9] Pech D, Brunet M, Durou H, Huang P, Mochalin V, Gogotsi Y, et al. Ultrahigh-power micrometre-sized supercapacitors based on onion-like carbon. Nat Nanotechnol. 2010 Sep;5(9):651-4.

[10] Liang J, Mondal AK, Wang D-W, Iacopi F. Graphene-Based Planar Microsupercapacitors: Recent Advances and Future Challenges. Adv Mater Technol. 2019;4(1):1800200.

[11] Lin J, Zhang C, Yan Z, Zhu Y, Peng Z, Hauge RH, et al. 3-Dimensional Graphene Carbon Nanotube Carpet-Based Microsupercapacitors with High Electrochemical Performance. Nano Lett. 2013 Jan 9;13(1):72-8.

[12] Kurra N, Jiang Q, Nayak P, Alshareef HN. Laser-derived graphene: A three-dimensional printed graphene electrode and its emerging applications. Nano Today. 2019 Feb 1;24:81-102.

[13] Si W, Yan C, Chen Y, Oswald S, Han L, Schmidt OG. On chip, all solid-state and flexible micro-supercapacitors with high performance based on MnOx/Au multilayers. Energy Environ Sci. 2013 Oct 18;6(11):3218-23.

[14] Brezesinski T, Wang J, Tolbert SH, Dunn B. Ordered mesoporous α -MoO 3 with iso-oriented nanocrystalline walls for thin-film pseudocapacitors. Nat Mater. 2010 Feb;9(2):146-51.

[15] Du J, Cheng H-M. The Fabrication, Properties, and Uses of Graphene/Polymer Composites. Macromol Chem Phys. 2012;213(10-11):1060-77.

[16] Kurra N, Xia C, N. Hedhili M, N. Alshareef H. Ternary chalcogenide micro-pseudocapacitors for on-chip energy storage. Chem Commun. 2015;51(52):10494-7.

[17] Naguib M, Kurtoglu M, Presser V, Lu J, Niu J, Heon M, et al.

Two-Dimensional Nanocrystals Produced by Exfoliation of Ti3AlC2. Adv Mater. 2011;23(37):4248-53.

[18] Naguib M, Mochalin VN, Barsoum MW, Gogotsi Y. 25th Anniversary Article: MXenes: A New Family of Two-Dimensional Materials. Adv Mater. 2014;26(7):992-1005.

[19] Anasori B, Lukatskaya MR, Gogotsi Y. 2D metal carbides and nitrides (MXenes) for energy storage. Nat Rev Mater. 2017 Jan 17;2(2):1-17.

[20] Zhan C, Sun W, Xie Y, Jiang D, Kent PRC. Computational Discovery and Design of MXenes for Energy Applications: Status, Successes, and Opportunities. ACS Appl Mater Interfaces. 2019 Jul 17;11(28):24885-905.

[21] Ghidiu M, Lukatskaya MR, Zhao M-Q, Gogotsi Y, Barsoum MW. Conductive two-dimensional titanium carbide 'clay' with high volumetric capacitance. Nature. 2014 Dec; 516(7529):78-81.

[22] Zhang Y, Wang L, Zhang N, Zhou Z. Adsorptive environmental applications of MXene nanomaterials: a review. RSC Adv. 2018 May 30;8(36):19895-905.

[23] Ibrahim Y, Mohamed A, Abdelgawad AM, Eid K, Abdullah AM, Elzatahry A. The Recent Advances in the Mechanical Properties of Self-Standing Two-Dimensional MXene-Based Nanostructures: Deep Insights into the Supercapacitor. Nanomaterials. 2020 Oct;10(10):1916.

[24] Tang H, Hu Q, Zheng M, Chi Y, Qin X, Pang H, et al. MXene–2D layered electrode materials for energy storage. Prog Nat Sci Mater Int. 2018 Apr 1; 28(2):133-47.

[25] Alhabeb M, Maleski K, Anasori B, Lelyukh P, Clark L, Sin S, et al. Guidelines for Synthesis and Processing of Two-Dimensional Titanium Carbide (Ti3C2Tx MXene). Chem Mater. 2017 Sep 26;29(18):7633-44.

[26] Li T, Yao L, Liu Q, Gu J, Luo R, Li J, et al. Fluorine-Free Synthesis of High-Purity Ti3C2Tx (T=OH, O) via Alkali Treatment. Angew Chem Int Ed. 2018; 57(21):6115-9.

[27] Peng C, Wei P, Chen X, Zhang Y, Zhu F, Cao Y, et al. A hydrothermal etching route to synthesis of 2D MXene (Ti3C2, Nb2C): Enhanced exfoliation and improved adsorption performance. Ceram Int. 2018 Oct 15;44(15):18886-93.

[28] Li M, Lu J, Luo K, Li Y, Chang K, Chen K, et al. Element Replacement Approach by Reaction with Lewis Acidic Molten Salts to Synthesize Nanolaminated MAX Phases and MXenes. J Am Chem Soc. 2019 Mar 20;141(11):4730-7.

[29] Sun W, Shah SA, Chen Y, Tan Z, Gao H, Habib T, et al. Electrochemical etching of Ti2AlC to Ti2CTx (MXene) in low-concentration hydrochloric acid solution. J Mater Chem A. 2017 Oct 24;5(41):21663-8.

[30] Yang S, Zhang P, Wang F, Ricciardulli AG, Lohe MR, Blom PWM, et al. Fluoride-Free Synthesis of Two-Dimensional Titanium Carbide (MXene) Using A Binary Aqueous System. Angew Chem Int Ed. 2018;57(47):15491-5.

[31] Khazaei M, Arai M, Sasaki T, Chung C-Y, Venkataramanan NS, Estili M, et al. Novel Electronic and Magnetic Properties of Two-Dimensional Transition Metal Carbides and Nitrides. Adv Funct Mater. 2013;23(17):2185-92.

[32] Khazaei M, Ranjbar A, Arai M, Sasaki T, Yunoki S. Electronic properties and applications of MXenes: a theoretical review. J Mater Chem C. 2017 Mar 9; 5(10):2488-503.

[33] Naguib M, Mashtalir O, Carle J, Presser V, Lu J, Hultman L, et al. Two-Dimensional Transition Metal Carbides.

ACS Nano. 2012 Feb 28;6(2): 1322-31.

[34] Zhang C (John), Anasori B, Seral-Ascaso A, Park S-H, McEvoy N, Shmeliov A, et al. Transparent, Flexible, and Conductive 2D Titanium Carbide (MXene) Films with High Volumetric Capacitance. Adv Mater. 2017;29(36): 1702678.

[35] Shahzad F, Alhabeb M, Hatter CB, Anasori B, Hong SM, Koo CM, et al. Electromagnetic interference shielding with 2D transition metal carbides (MXenes). Science. 2016 Sep 9; 353(6304):1137-40.

[36] Alnoor H, Elsukova A, Palisaitis J, Persson I, Tseng EN, Lu J, et al. Exploring MXenes and their MAX phase precursors by electron microscopy. Mater Today Adv. 2021 Mar 1;9:100123.

[37] Wang H-W, Naguib M, Page K, Wesolowski DJ, Gogotsi Y. Resolving the Structure of Ti3C2Tx MXenes through Multilevel Structural Modeling of the Atomic Pair Distribution Function. Chem Mater. 2016 Jan 12;28(1):349-59.

[38] Wang X, Shen X, Gao Y, Wang Z, Yu R, Chen L. Atomic-Scale Recognition of Surface Structure and Intercalation Mechanism of Ti3C2X. J Am Chem Soc. 2015 Feb 25;137(7):2715-21.

[39] Khazaei M, Arai M, Sasaki T, Estili M, Sakka Y. Two-dimensional molybdenum carbides: potential thermoelectric materials of the MXene family. Phys Chem Chem Phys. 2014 Apr 2;16(17) :7841-9.

[40] Shein IR, Ivanovskii AL. Graphene-like titanium carbides and nitrides Tin+1Cn, Tin+1Nn (n=1, 2, and 3) from de-intercalated MAX phases: First-principles probing of their structural, electronic properties and relative stability. Comput Mater Sci. 2012 Dec 1;65:104-14.

[41] Gao G, Ding G, Li J, Yao K, Wu M, Qian M. Monolayer MXenes: promising half-metals and spin gapless semi-conductors. Nanoscale. 1395 Feb 2;8(16):8986-94.

[42] Khazaei M, Ranjbar A, Ghorbani-Asl M, Arai M, Sasaki T, Liang Y, et al. Nearly free electron states in MXenes. Phys Rev B. 2016 May 16;93(20):205125.

[43] Lee Y, Cho SB, Chung Y-C. Tunable Indirect to Direct Band Gap Transition of Monolayer Sc2CO2 by the Strain Effect. ACS Appl Mater Interfaces. 2014 Aug 27;6(16):14724-8.

[44] Plummer G, Anasori B, Gogotsi Y, Tucker GJ. Nanoindentation of monolayer Tin+1CnTx MXenes via atomistic simulations: The role of composition and defects on strength. Comput Mater Sci. 2019 Feb 1;157:168-74.

[45] Borysiuk VN, Moachalin VN, Gogotsi Y. Molecular dynamic study of the mechanical properties of two-dimensional titanium carbides Tin+ 1Cn (MXenes). Nanotechnology. 2015 Jun;26(26):265705.

[46] Ling Z, Ren CE, Zhao M-Q, Yang J, Giammarco JM, Qiu J, et al. Flexible and conductive MXene films and nano-composites with high capacitance. Proc Natl Acad Sci. 2014 Nov 25;111(47): 16676-81.

[47] Jiang Q, Kurra N, Maleski K, Lei Y, Liang H, Zhang Y, et al. On-Chip MXene Microsupercapacitors for AC-Line Filtering Applications. Adv Energy Mater. 2019;9(26):1901061.

[48] Kim E, Lee B-J, Maleski K, Chae Y, Lee Y, Gogotsi Y, et al. Micro-supercapacitor with a 500 nm gap between MXene/CNT electrodes. Nano Energy. 2021 Mar 1;81:105616.

[49] Liu N, Gao Y. Recent Progress in Micro-Supercapacitors with In-Plane

Interdigital Electrode Architecture. Small. 2017;13(45):1701989.

[50] Xu S, Wei G, Li J, Ji Y, Klyui N, Izotov V, et al. Binder-free Ti3C2Tx MXene electrode film for supercapacitor produced by electrophoretic deposition method. Chem Eng J. 2017 Jun 1;317: 1026-36.

[51] Begines B, Alcudia A, Aguilera-Velazquez R, Martinez G, He Y, Trindade GF, et al. Design of highly stabilized nanocomposite inks based on biodegradable polymer-matrix and gold nanoparticles for Inkjet Printing. Sci Rep. 2019 Nov 6;9(1):16097.

[52] Zhang C (John), McKeon L, Kremer MP, Park S-H, Ronan O, Seral-Ascaso A, et al. Additive-free MXene inks and direct printing of micro-supercapacitors. Nat Commun. 2019 Apr 17;10(1):1795.

[53] Wu C-W, Unnikrishnan B, Chen I-WP, Harroun SG, Chang H-T, Huang C-C. Excellent oxidation resistive MXene aqueous ink for micro-supercapacitor application. Energy Storage Mater. 2020 Mar 1;25:563-71.

[54] Tang J, Yi W, Zhong X, Zhang C (John), Xiao X, Pan F, et al. Laser writing of the restacked titanium carbide MXene for high performance supercapacitors. Energy Storage Mater. 2020 Nov 1;32:418-24.

[55] Wang N, Liu J, Zhao Y, Hu M, Qin R, Shan G. Laser-Cutting Fabrication of Mxene-Based Flexible Micro-Supercapacitors with High Areal Capacitance. ChemNanoMat. 2019;5(5):658-65.

[56] Kurra N, Ahmed B, Gogotsi Y, Alshareef HN. MXene-on-Paper Coplanar Microsupercapacitors. Adv Energy Mater. 2016;6(24):1601372.

[57] Abdolhosseinzadeh S, Jiang X, Zhang H, Qiu J, Zhang C (John). Perspectives on solution processing of two-dimensional MXenes. Materials Today. 2021 Mar 15.

[58] Abdolhosseinzadeh S, Schneider R, Verma A, Heier J, Nüesch F, Zhang C (John). Turning Trash into Treasure: Additive Free MXene Sediment Inks for Screen-Printed Micro-Supercapacitors. Adv Mater. 2020;32(17):2000716.

[59] Xu S, Dall'Agnese Y, Wei G, Zhang C, Gogotsi Y, Han W. Screen-printable microscale hybrid device based on MXene and layered double hydroxide electrodes for powering force sensors. Nano Energy. 2018 Aug 1;50:479-88.

[60] Orangi J, Hamade F, Davis VA, Beidaghi M. 3D Printing of Additive-Free 2D Ti_3C_2Tx (MXene) Ink for Fabrication of Micro-Supercapacitors with Ultra-High Energy Densities. ACS Nano. 2020 Jan 28;14(1):640-50.

[61] Yang W, Yang J, Byun JJ, Moissinac FP, Xu J, Haigh SJ, et al. 3D Printing of Freestanding MXene Architectures for Current-Collector-Free Supercapacitors. Adv Mater. 2019; 31(37):1902725.

[62] Quain E, Mathis TS, Kurra N, Maleski K, Aken KLV, Alhabeb M, et al. Direct Writing of Additive-Free MXene-in-Water Ink for Electronics and Energy Storage. Adv Mater Technol. 2019;4(1): 1800256.

[63] Zhang C (John), Kremer MP, Seral-Ascaso A, Park S-H, McEvoy N, Anasori B, et al. Stamping of Flexible, Coplanar Micro-Supercapacitors Using MXene Inks. Adv Funct Mater. 2018; 28(9):1705506.

[64] Hu H, Hua T. An easily manipulated protocol for patterning of MXenes on paper for planar micro-supercapacitors. J Mater Chem A. 2017 Sep 26;5(37): 19639-48.

[65] Li P, Shi W, Liu W, Chen Y, Xu X, Ye S, et al. Fabrication of

high-performance MXene-based all-solid-state flexible microsupercapacitor based on a facile scratch method. Nanotechnology. 2018 Sep;29(44):445401.

[66] Li J, Levitt A, Kurra N, Juan K, Noriega N, Xiao X, et al. MXene-conducting polymer electrochromic microsupercapacitors. Energy Storage Mater. 2019 Jul 1;20:455-61.

[67] Chen X, Wang S, Shi J, Du X, Cheng Q, Xue R, et al. Direct Laser Etching Free-Standing MXene-MoS2 Film for Highly Flexible Micro-Supercapacitor. Adv Mater Interfaces. 2019;6(22):1901160.

[68] Peng Y-Y, Akuzum B, Kurra N, Zhao M-Q, Alhabeb M, Anasori B, et al. All-MXene (2D titanium carbide) solid-state microsupercapacitors for on-chip energy storage. Energy Environ Sci. 2016 Aug 31;9(9):2847-54.

[69] Salles P, Quain E, Kurra N, Sarycheva A, Gogotsi Y. Automated Scalpel Patterning of Solution Processed Thin Films for Fabrication of Transparent MXene Microsupercapacitors. Small. 2018;14(44):1802864.

[70] Li Q, Wang Q, Li L, Yang L, Wang Y, Wang X, et al. Femtosecond Laser-Etched MXene Microsupercapacitors with Double-Side Configuration via Arbitrary On- and Through-Substrate Connections. Adv Energy Mater. 2020;10(24):2000470.

[71] Huang X, Wu P. A Facile, High-Yield, and Freeze-and-Thaw-Assisted Approach to Fabricate MXene with Plentiful Wrinkles and Its Application in On-Chip Micro-Supercapacitors. Adv Funct Mater. 2020;30(12):1910048.

[72] Zhang L, Yang G, Chen Z, Liu D, Wang J, Qian Y, et al. MXene coupled with molybdenum dioxide nanoparticles as 2D-0D pseudocapacitive electrode for high performance flexible asymmetric micro-supercapacitors. J Materiomics. 2020 Mar 1;6(1):138-44.

[73] Huang H, Su H, Zhang H, Xu L, Chu X, Hu C, et al. Extraordinary Areal and Volumetric Performance of Flexible Solid-State Micro-Supercapacitors Based on Highly Conductive Freestanding Ti3C2Tx Films. Adv Electron Mater. 2018;4(8):1800179.

[74] Huang H, Chu X, Su H, Zhang H, Xie Y, Deng W, et al. Massively manufactured paper-based all-solid-state flexible micro-supercapacitors with sprayable MXene conductive inks. J Power Sources. 2019 Mar 1;415:1-7.

[75] Yue Y, Liu N, Ma Y, Wang S, Liu W, Luo C, et al. Highly Self-Healable 3D Microsupercapacitor with MXene–Graphene Composite Aerogel. ACS Nano. 2018 May 22;12(5):4224-32.

[76] Couly C, Alhabeb M, Aken KLV, Kurra N, Gomes L, Navarro-Suárez AM, et al. Asymmetric Flexible MXene-Reduced Graphene Oxide Micro-Supercapacitor. Adv Electron Mater. 2018;4(1):1700339.

[77] Yu C, Gong Y, Chen R, Zhang M, Zhou J, An J, et al. A Solid-State Fibriform Supercapacitor Boosted by Host–Guest Hybridization between the Carbon Nanotube Scaffold and MXene Nanosheets. Small. 2018;14(29): 1801203.

[78] Yang Q, Xu Z, Fang B, Huang T, Cai S, Chen H, et al. MXene/graphene hybrid fibers for high performance flexible supercapacitors. J Mater Chem A. 2017 Oct 31;5(42):22113-9.

[79] Li H, Li X, Liang J, Chen Y. Hydrous RuO2-Decorated MXene Coordinating with Silver Nanowire Inks Enabling Fully Printed Micro-Supercapacitors with Extraordinary Volumetric Performance. Adv Energy Mater. 2019;9(15):1803987.

[80] Wang Y, Wang X, Li X, Bai Y, Xiao H, Liu Y, et al. Scalable fabrication of polyaniline nanodots decorated MXene film electrodes enabled by viscous functional inks for high-energy-density asymmetric supercapacitors. Chem Eng J. 2021 Feb 1;405:126664.

[81] Jiao S, Zhou A, Wu M, Hu H. Kirigami Patterning of MXene/Bacterial Cellulose Composite Paper for All-Solid-State Stretchable Micro-Supercapacitor Arrays. Adv Sci. 2019;6(12):1900529.

[82] Shao W, Tebyetekerwa M, Marriam I, Li W, Wu Y, Peng S, et al. Polyester@MXene nanofibers-based yarn electrodes. J Power Sources. 2018 Aug 31;396:683-90.

[83] Zhang J, Seyedin S, Gu Z, Yang W, Wang X, Razal JM. MXene: a potential candidate for yarn supercapacitors. Nanoscale. 2017 Dec 7;9(47):18604-8.

[84] He N, Liao J, Zhao F, Gao W. Dual-Core Supercapacitor Yarns: An Enhanced Performance Consistency and Linear Power Density. ACS Appl Mater Interfaces. 2020 Apr 1;12(13):15211-9.